Using Symmetry to Detect Abnormalities in Brain MRI

Nilanjan Ray[1], Russell Greiner[1] and Albert Murtha[2]
{nray1, greiner}@cs.ualberta.ca, albertmu@cancerboard.ab.ca

[1]Department of Computing Science
University of Alberta, Edmonton, AB, Canada

[2]Division of Radiation Oncology
[2]Department of Oncology
University of Alberta, Edmonton, AB, Canada

Abstract
Automated tumor segmentation from magnetic resonance imagery (MRI) plays a significant role in cancer research and clinical practice. However, tumor segmentation is an extremely challenging task: clinicians believe that a gamut of prior domain knowledge and clinical data should be used, along with the MR image. As a step toward tumor segmentation, we illustrate here a real-time algorithm to locate the brain abnormality in an MR image by putting a bounding box around it. Our approach is based on left-to-right symmetry of the brain. In additional to being real-time, some advantages of the proposed algorithm are: (a) it requires no registration of MR images, (b) it needs no training image and (c) it is independent of intensity variations across MR images. Our detection algorithm can play a useful role in indexing and storage of MRI data and as an initial step toward accurate tumor boundary delineation.

Introduction

Automated tumor segmentation from brain MR (magnetic resonance) images can play a significant role in medical research and clinical practice. Many clinical centers currently maintain large amounts of archived Magnetic Resonance (MR) images of brain tumors. Unless these images are segmented, however, it is difficult retrieve the relevant images, for analysis – e.g., allowing a clinician to use tumor location to retrieve historical cases relevant to the diagnosis and treatment of cancers in new patients. Moreover, radiologists currently segment patients' tumors by hand on MR images before applying a treatment such as radiation therapy. This manual segmentation process is laborious and expensive.

Automatically segmenting tumors in brain MRI is an extremely challenging task. For an account of this topic from image analysis and machine learning perspective, see [7]. There are many challenges here, many corresponding to the challenge of incorporating domain knowledge. On the computational front, pixel labeling algorithms, such as support vector classifiers, which learn local features (computed within a window around a pixel), are not adequate to segment brain abnormality (tumor, edema, etc.). On the other hand, incorporation of global region-based features is non-trivial and computationally intensive [2]. Attempts have also been made to incorporate pixel classification and region similarity (see [2], [5]).

In this paper we describe a fast method for locating a bounding box around the region of abnormality. The algorithm is suitable for indexing tumor images for archival and retrieval purposes. In database applications the typical query will be based on the location of the tumor as well as the size of the tumor; both of which can be approximately indicated by the bounding box created by the proposed algorithm. This approach can also help to find an accurate segmentation boundary, as we later illustrate. Our method exploits the facts that a normal brain structure is symmetric – the left part and the right part can be divided by an axis of symmetry, and abnormalities (tumors, edema) typically disturb this symmetry. However, note that the symmetry is only approximate, even if the axis of symmetry is found correctly. Moreover, finding the axis of symmetry accurately is difficult. Thus, we carefully exploit the approximate left-right symmetry in our algorithm, which is, to a good extent, resilient to the error in locating the axis of symmetry. We next define the proposed technique, first presented earlier in [6].

Proposed Technique

Consider the change detection problem: find the region of abnormality D from image I using a reference (or template) image R that does not involve any abnormalities (Fig. 1(a)). An obvious way would be to compare the images I and R point-wise, looking at the absolute point-wise difference image $|I-R|$. If R matches with I everywhere except within the region D, then $|I-R|$ is a good pattern image to detect the region D. In the real world, the difference image $|I-R|$ is quite noisy; moreover the available reference image R almost never matches with I by point-wise comparisons. In other words, it is often the case that

the available template image R matches I *approximately*, and only after applying displacements: $R(x+f(x,y), y+g(x,y)) \approx I(x,y)$, where $f(x, y)$ and $g(x, y)$ are respectively the x and y displacements; n.b. these are not constants, but vary with the (x, y) position. If one can reliably estimate these unknown displacement functions f and g, then our original problem of finding the region D can be solved by forming the aforementioned difference image *after* applying f and g to the domain of the template image R: $|R(x+f(x,y), y+g(x,y)) - I(x,y)|$. However, finding the displacement functions is certainly a non-trivial problem and (we will see) is not necessary for the aforementioned detection problem.

We detect the abnormal region D by using image intensity histograms from I and R. Our approach completely avoids computing the displacement functions f and g, which is a major advantage as we believe determining these functions is much more difficult than the original detection problem. To help illustrate our algorithm, consider Fig. 1(a), with a horizontal dotted line drawn at a distance s from the top of the images. Now consider the regions: $A(s) = [0, w] \times [0, s]$, and $B(s) = [0, w] \times [s, h]$, where w and h are respectively the width and the height of both the images I and R. Thus $A(s)$ and $B(s)$ are the portions of image domain respectively above and below the aforementioned horizontal line. Let $E(s)$ denote the following score function:

$$E(s) = \langle \sqrt{P_I^{A(s)}}, \sqrt{P_R^{A(s)}} \rangle - \langle \sqrt{P_I^{B(s)}}, \sqrt{P_R^{B(s)}} \rangle,$$

where P's denote normalized intensity histograms (probability mass functions of image intensities), the subscripts indicate whether this histogram is of image I or of template R, and the superscripts denote whether this histogram is computed within the region $T(s)$ or within the region $B(s)$. For example, $P_I^{T(s)}$ denotes the normalized intensity histogram of image I within $A(s)$. $\langle X, Y \rangle$ denotes the inner product (*i.e.*, sum of element-wise product) between two vectors X and Y. The inner product between square roots of two normalized histograms is known as Bhattacharya coefficient (BC), [4] which is a real number between 0 and 1 that measures the correlation between two histograms. When two normalized histograms are identical, their BC value is 1; whereas when the histograms are completely different, their BC value is 0.

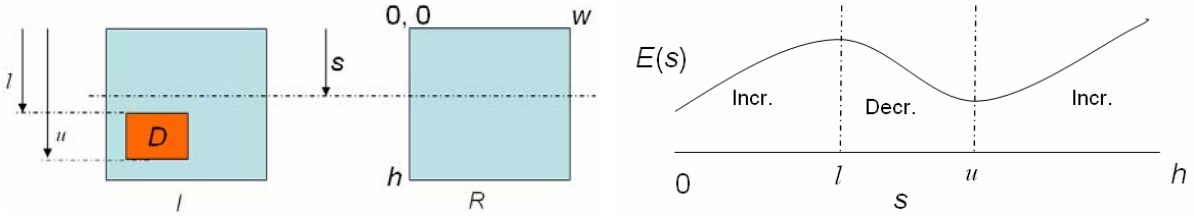

(a) (b)

Fig 1: (a) Finding D from image I, using a reference image R, (b) A typical score function plot.

Note that the score function $E(s)$ measures the difference of correlations between the upper histograms and the lower histograms. We therefore expect a high score when the upper histograms match very well, while the lower histograms have high mismatch. On the other hand, a low value of $E(s)$ denotes a low correlation between upper histograms, and a high correlation between lower histograms. Based on these observations, we note that a plot of $E(s)$ vs. s should look like the plot shown in Fig. 1(b). The important observations in Fig. 1(b) are that the plot has three distinct regions – increasing, decreasing, then increasing – where the decreasing segment begins at l and ends at u, where l and u respectively denotes the lower and the upper bound for the rectangular region D, measuring from top of the image. In fact we can prove these statements rigorously with some mild assumptions about the data, *i.e.*, about the image I and the template R. Essentially, we require that the correlation between the image histogram *outside* D and the template histogram is much larger than that between the image histogram *inside* D and the template histogram:

$$(i) \quad \langle \sqrt{P_I^{A(s)\cap D}}, \sqrt{P_R^{A(s)}} \rangle << \langle \sqrt{P_I^{A(s)\setminus D}}, \sqrt{P_R^{A(s)}} \rangle, \quad (ii) \quad \langle \sqrt{P_I^{B(s)\cap D}}, \sqrt{P_R^{B(s)}} \rangle << \langle \sqrt{P_I^{B(s)\setminus D}}, \sqrt{P_R^{B(s)}} \rangle.$$

Without these assumptions the abnormal region D would look like rest of the image I, and it would be difficult (if not impossible) to detect D then. For brevity of space, here we omit the proof [6].

Our task is to find the maximum and the minimum points of the plot corresponding to the lower and the upper bounds of region D (Fig. 1(b)). Thus, algorithmically, a vertical sweep of the image I and R

finds the upper and lower bounds of *D*. Similarly, a horizontal sweep and a similar plot of the score function help find out the left and the right bound for *D*. The plots from this procedure appear in Fig 2. The upper left picture shows a brain MRI with an abnormality on the left of the image. In general, we assume the input image is an axial slice, which is close to being vertical. We first detect the skull boundary by active contour algorithm [8]. Next an ellipse is fitted to the skull boundary, from which we extract the line of symmetry (shown on the upper right picture of Fig. 2). Then we treat *I* as the image formed by the portion to the left of the line of symmetry and *R* as the portion of the image to right of the line of symmetry after taking a reflection. Next, a vertical sweep and a horizontal sweep produce the score plots respectively shown on the lower left and lower right pictures in Fig. 2. The maxima and the minima are detected from these two plots, and the corresponding bounding box is overlaid on the upper left picture of Fig. 2.

Results

In this section we show some results of applying our algorithm to brain MRI data. Fig. 3 shows four MR images with bounding boxes found by our algorithm. These bounding boxes are seen to be crudely segmenting the abnormalities.

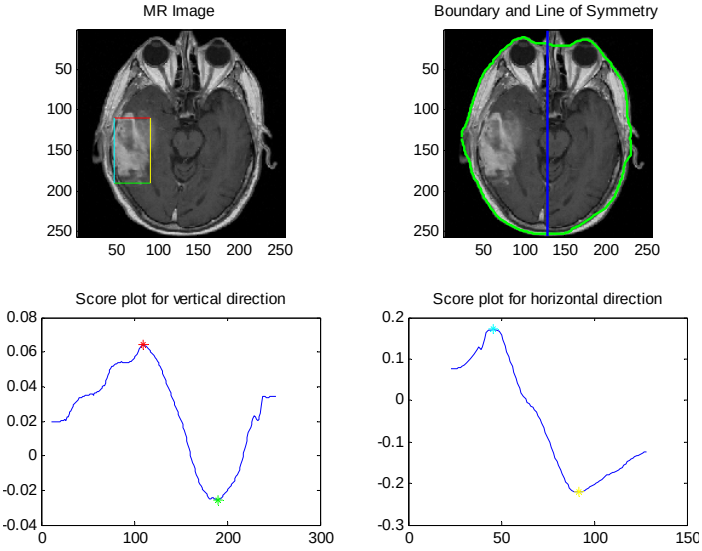

Fig 2: Finding a bounding box on brain MRI.

To quantify the performance of our algorithm we use Dice coefficient [3]:

$$Dice\ Coefficient = \frac{2|G \cap S|}{|G| + |S|},$$

where *G* is the set of the pixels of a bounding box around the true abnormality (here, found by an expert radiologist) and *S* is set of pixels of the bounding box found by our algorithm. The modulus sign appearing in the Dice coefficient expression denotes cardinality (number of pixels in this case) of a set. In general, the Dice coefficient is a value between 0 and 1, with 1 being the ideal segmentation, *S*=*G*. The closer the Dice coefficient is to unity, the better the segmentation is. Fig. 4 shows encouraging Dice coefficient values for two sets of brain MRI data taken from studies on two patients.

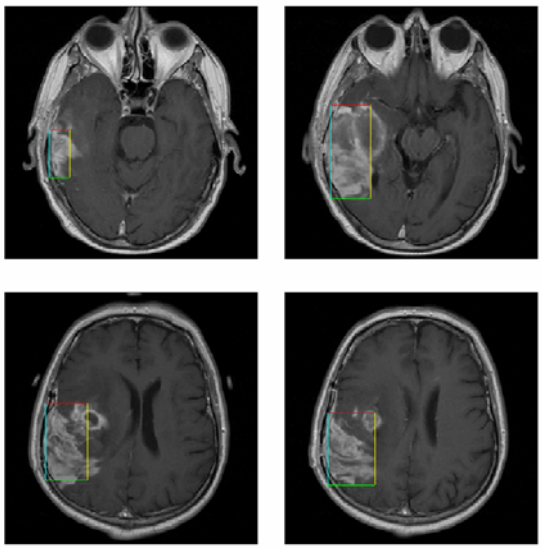

Fig 3: MR images and bounding boxes around abnormal regions.

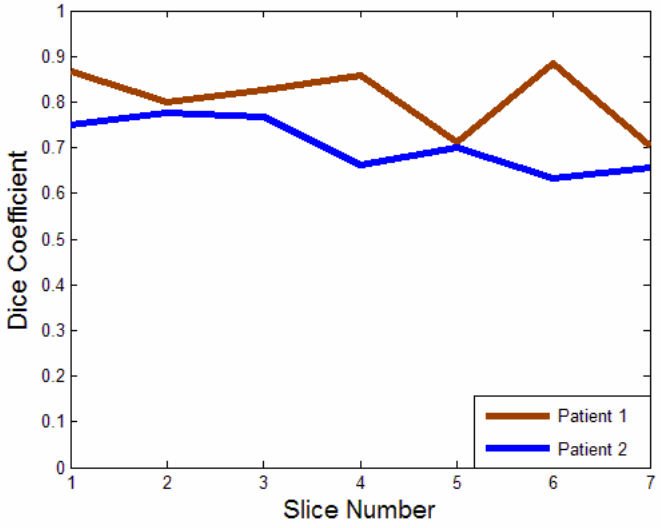

Fig 4: Dice coefficients for MR images for two studies.

As mentioned before, the proposed bounding box algorithm only provides a rough estimate of the abnormal region. However, after finding the bounding box, we can fine tune the segmentation boundary as shown in Fig. 5. Fig. 5(a) shows the bounding box found by our algorithm. Fig. 5(b) shows the result of the Chan-Vese [1] segmentation algorithm applied *only within the bounding box*. On the other hand, Fig. 5(c) shows the result of Chan-Vese algorithm applied *on the entire image*. While in Fig. 5(b) the segmentation boundary is confined to the correct region of abnormality, in Fig. 5(c) spurious segmentation boundaries are created. This example shows that our proposed bounding box algorithm can aid in delineating the boundary of the region of abnormality.

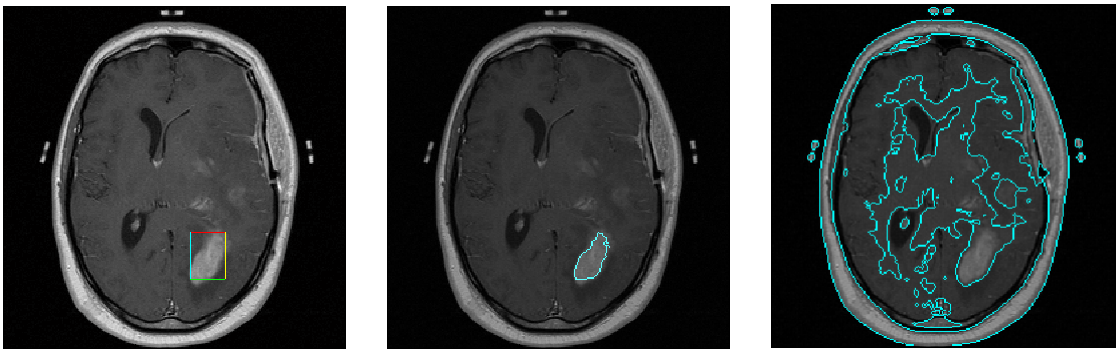

(a) (b) (c)

Fig 5: (a) Bounding box, (b) segmentation within bounding box, (c) segmentation on the entire image.

Future Work and Conclusions

This work provides an effective scoring function that helps locate abnormalies in brain MR images. This approach can open new avenues for brain tumor segmentation. The principal advantages of the proposed algorithm are that it (a) exploits approximate left-right symmetry of brain, (b) uses only a single MR image, so there is no effect of variability in image intensity across MR images, (c) needs no training data, (d) requires no image registration, and (e) can be implemented in real-time.

Inspired by some encouraging initial results, in the future we plan to extensively test our algorithm on the Cross Cancer Institute image database. As indicated we also will incorporate this algorithm as a pre-processing step at in-house segmentation algorithms (visit: http://www.cs.ualberta.ca/~btgp/). We also plan to extend this to 3-dimensions.

We are seeking other applications where our algorithm can be successfully deployed. One such area is video surveillance. Because of histogram-based score function, we hope our method can accommodate the effects of jitters and considerable camera motion in a surveillance video that poses a tremendous challenge to the state-of-the-art background subtraction/change detection methods.

References

[1] T.F. Chan and L.A. Vese, "Active contours without edges," *IEEE Transactions on Image Processing*, vol.10, no.2, pp.266-277, 2001.

[2] D. Cobzas, N. Birkbeck, M. Schmidt, M. Jägersand, A. Murtha, "3D variational brain tumor segmentation using a high dimensional feature set," In *Mathematical Methods in Biomedical Image Analysis*, a workshop in conjunction with International Conference on Computer Vision (ICCV 2007), Rio de Janeiro, Brazil, October 2007.

[3] L.R. Dice, "Measures of the amount of ecologic association between species," *Ecology*, vol. 26, pp.297-302, 1945.

[4] K. Fukunaga, *Introduction to statistical pattern recognition*, Academic Press, 2nd ed., 1990.

[5] C-H. Lee, S. Wang, F. Jiao, R. Greiner, D. Schuurmans, "Learning to model spatial dependency: semi-supervised discriminative random fields," *Neural Information Processing Systems*. Vancouver, BC. December 2006.

[6] N. Ray, B. Saha, M. Brown, "Locating brain tumor from MR imagery using symmetry," accepted at *Asilomar conf. on signals, systems, and computers*, Pacific Grove, California, USA, 2007.

[7] M. Schmidt, *Automatic brain tumor segmentation*, M.Sc. Thesis, University of Alberta, 2005.

[8] C. Xu and J. L. Prince, "Snakes, shapes, and gradient vector flow," *IEEE Transactions on Image Processing*, vol.7, no.3, pp.359-369, 1998.

Nilanjan Ray received his bachelor degree in mechanical engineering from Jadavpur University, Calcutta, India, in 1995, master's degree in computer science from the Indian Statistical Institute, Calcutta, in 1997, and Ph.D. in electrical engineering from the University of Virginia, Charlottesville, in 2003. Following a post doctoral and an industrial position, he joined the department of Computing Science, University of Alberta in July 2006. Nilanjan is a recipient of the CIMPA-UNESCO fellowship for image processing in 1999; the graduate fellowship at Indian Statistical Institute from 1995 to 1997; and the best student paper award from IBM Picture Processing Society presented at the IEEE International Conference on Image Processing, Rochester, NY, 2002. Nilanjan's research area is image analysis and computer vision.

After earning a PhD from Stanford, Russ Greiner worked in both academic and industrial research before settling at the University of Alberta, where he is now a Professor in Computing Science and the Scientific Director of the Alberta Ingenuity Centre for Machine Learning, which won the ASTech Award for "Outstanding Leadership in Technology" in 2006. He has been Program Chair for the 2004 "Int'l Conf. on Machine Learning", Conference Chair for 2006 "Int'l Conf. on Machine Learning", Editor-in-Chief for "Computational Intelligence", and is serving on the editorial boards of a number of other journals. He was elected a Fellow of the AAAI (Association for the Advancement of Artificial Intelligence) in 2007, and was awarded a McCalla Professorship in 2005-06 and a Killam Professorship in 2007. He has published over 100 refereed papers and patents, most in the areas of machine learning and knowledge representation. The main foci of his current work are (1) bioinformatics and medical informatics; (2) learning effective probabilistic models and (3) formal foundations of learnability.

Albert Murtha, MD, FRCPC, is an associate professor in the Division of Radiation Oncology and the Division of Experimental Oncology at Cross Cancer Institute, University of Alberta. His clinical interests include neuro-oncology (Tumour Group Leader), Prostate Brachytherapy, and Hematological Malignancies. His research interest spans across topics such as, Machine Learning (Artificial Intelligence) as applied to the treatment of cancer, normal tissue tolerance to radiation therapy, high field MRI and PET scanning for prediction of tumour/normal tissue response to radiation therapy, and low dose rate radiobiology.